

Investigation of electronic and optical properties of nano-Ag produced from heterocyclic compounds by green chemistry reactions

Asli Ozturk Kiraz^{1,*}, Mine Sulak², Yesim Kara³, Izzet Kara²

¹Department of Physics, Faculty of Science & Letters, Pamukkale University, Denizli, Türkiye

²Pamukkale University, Faculty of Education, Department of Maths. and Science Education, Denizli, Türkiye

³Department of Biology, Faculty of Science, Pamukkale University, Kınıklı Campus, 20070, Denizli, Türkiye

Abstract: The synthesis of nanoparticles using biological molecules has become one of the current research areas due to the high toxic content, poor stability, and expensive production technologies of nanoparticles synthesized by physical and chemical technologies. With the approach called green synthesis, nanoparticles that do not contain toxic substances have been produced in a method that does not harm the environment and human health. The number of polyphenol compounds in the ethyl alcohol/water extract of propolis collected from the Muğla-Türkiye region was determined. The synthesis and characterization of silver nanoparticles were carried out using the ethyl alcohol/water extract of propolis. The descriptions of the synthesized nanoparticles were made using ultraviolet-visible absorption and attenuated total reflection-Fourier transform infrared. Scanning electron microscopy, energy-dispersive X-ray, and X-ray diffraction methods were used for morphological examinations. Which polyphenol compound in the propolis content is effective in the synthesis of nanosilver particles was investigated with a Gaussian 16 package program. The electronic properties of the compounds were obtained by density functional theory using boundary orbitals theory, molecular electrostatic surface potential, and nonlinear optical properties. Epigallocatechin gallate, Kaempferol, and Quercetin are effective in obtaining nano-Ag and can be used as organic optical material in technology.

ARTICLE HISTORY

Received: May 17, 2023

Revised: Oct. 09, 2023

Accepted: Oct. 12, 2023

KEYWORDS

Propolis,
Green chemistry,
Nano-Ag,
Density functional theory,
Non-linear optical
properties.

1. INTRODUCTION

The word “nano”, whose etymological origin is based on Greek. A nanometer (nm) is a unit of length in the metric system that equals one billionth of a meter. It is a very small dimensional quantity that is beyond our perceptual limits. However, through nanoscience, we can understand the new behaviors of non-standard nanometric materials on the nanometer scale with the help of quantum theory. On the other hand, nanotechnology allows us to engineer matter on an atomic-molecular scale to unleash brand-new properties. Nanotechnology is a cutting-edge field that confidently pursues the creation of functional materials, devices, and systems that have the ability to manipulate, control, and produce physical, chemical, and biological

*CONTACT: Asli Ozturk Kiraz ✉ aslio@pau.edu.tr 📧 Department of Physics, Faculty of Science & Letters, Pamukkale University, Denizli, Türkiye

phenomena at the atomic and molecular scale. Its precision and accuracy in achieving these goals make it an exciting and promising area of research. (Santhoshkumar *et al.*, 2017; Das *et al.*, 2009).

Metallic nanoparticles or metal nanoparticles have emerged as new terminology in the nanoparticulate field over the past few years. Noble metals such as gold, silver, and platinum, which are biocompatible, are used for the synthesis of metal nanoparticles (Hojat *et al.*, 2018). Different physical and chemical methods such as electrochemical changes, chemical reduction, and photochemical reduction are widely used for the preparation and stabilization of metal nanoparticles (Geethalakshmi R *et al.*, 2012). One of the most remarkable metal nanoparticles is silver nanoparticles. Silver nanoparticles have several specific properties such as catalysis, magnetic and optical polarization, electrical conductivity, and microbial activity. Silver nanoparticles show a unique optical property because they support surface plasmons.

Numerous methods have been developed for the synthesis of silver nanoparticles in a solution medium. The most used methods are chemical precipitation, photochemical, electrochemical alcoholic reduction, polyol, solgel, microemulsion, etc. such as chemical methods (Bhattacharya *et al.*, 2008). The use of chemical and physical methods in the synthesis of nanoparticles is very expensive and laborious and also leads to the presence of some toxic chemicals on the surface that harms the environment in applications (Siddiquee *et al.*, 2020). Green synthesis used for metal nanoparticle synthesis is a biological approach using proteins, microorganisms, plants, or plant extracts, which has been proposed as an alternative to chemical methods. In the biosynthetic method, toxic chemicals are not used and the need for high pressure, energy, and temperature is not felt.

Propolis is a natural bee product that is used for many purposes in the hive, containing a mixture of wax, and resin, enriched with wax, pollen, and saliva secretions, which bees collect from the buds and bark of flowers and deciduous trees. Many scientific studies have shown that propolis has been used in the treatment of various diseases in traditional medicine since ancient times and has biological activities such as antimicrobial, antioxidant, antitumor, anti-inflammatory, and antiulcer. The structure and content of propolis vary according to the variety of plants that bees can reach. The physical properties of propolis, such as its chemical composition, also vary depending on the geographical structure and climate of the region where it is collected (Krell, 1996). The most important pharmacologically active components in propolis are flavonoids, flavanols, flavanones, alkaloids, steroids, terpenoids, and various phenolic and aromatics, followed by hydroxycinnamic acids such as caffeic, ferulic, acid, and caffeic acid phenyl esters (Petri *et al.*, 1988). It has been reported in previous studies that it is used in the synthesis of nanoparticles due to these large biomolecular compounds in bee propolis (Ramnath, 2017; Padil *et al.*, 2013). The proportions of biomolecular compounds in propolis vary considerably depending on the flower and tree structure in the region where the bee is located.

In this study, phenols contained in the ethanol extract of bee propolis collected from the province of Mugla-Türkiye were used as reducing and stabilizing agents for the biosynthesis of silver nanoparticles (P-AgNPs). The phenol and flavonoid contents of the ethyl alcohol extract of the propolis we have were analyzed. After determining the component amounts of the substances in propolis, computer calculations were used to understand which substance was effective in the synthesis of silver nanoparticles. The resulting nanoparticles were further characterized by UV-Vis, FTIR, EDX, SEM, and XRD analysis.

Density Functional Theory (DFT) is a very important method in fundamental sciences such as physics, chemistry, and biology since it gives a lot of information about the electronic structure of materials (Van Mourik *et al.*, 2014). In addition, the development of computer performance in recent years has led to the use of this method more effectively. Thus, it enabled

more experimental and computational studies to be carried out compared to 15-20 years ago. DFT calculations provide structural, force, and total energy information as well as system charge density. These features provide comparison and connection with experiments and identification of underlying mechanisms through the analysis of the electronic structure (Mason *et al.*, 2010).

2. MATERIAL and METHODS

2.1. Material

Silver nitrate (AgNO₃) and sodium hydroxide (NaOH) chemicals used to obtain silver nanoparticles were obtained from Sigma-Aldrich, Inc. (St. Louis, MO, USA). All reagents and solvents used in antioxidant activity determinations are of analytical purity and used Folin-Ciocalteu reagent Sigma-Aldrich Chemie, Munich, Germany), TPTZ (tripridyltriazine) Merck (Darmstadt, Germany), Trolox (6-hydroxy-2,5,7,8-tetramethylchroman-2-carboxylic acid) from Sigma Aldrich and HCl, ethanol from Merck (Darmstadt, Germany). Shaker Heidolph MR HEI-Standard (Schwabach, Germany) mixer Vortex Mixer Labnet VX100, MO BIO Laboratories, Inc. (NJ, USA) instruments were used for extraction. In addition, Spectro UV-Vis Double Beam PC LaboMed Inc., (Los Angeles, CA, USA) was preferred in UV-VIS spectrophotometer for antioxidant activity measurements. Rotary evaporator with hood IKA®-Werke, RV 05 Basic (Staufen, Germany) was used.

2.2. Preparation of Propolis Extract

Approximately 5 g of propolis collected from the region was taken and kept in a shaker (Heidolph Shaker, Schwabach, Germany) for 24 hours for the preparation of ethanol/water (1:1 v/v) extracts. In order to purify the solid particles in the solution, filtration was carried out using ordinary filter paper first and then blue band filter paper. Concentrations were determined by adjusting the final volumes. Stock solutions were kept at +4°C until the analysis period.

2.3. The Total Amount of Phenolic Substance

The total phenolic content of ethanol/water extracts of crude propolis samples was determined according to the method developed by Slinkard and Singleton (Slinkard *et al.*, 1977). For this purpose, a standard calibration curve was prepared using the gallic acid standard. For this, different concentrations of gallic acid (500; 250; 125; 62.5; 31.25, and 15.625 µg/mL) were prepared and read at 760 nm by pipetting and incubating with Folin-Ciocalteu reagent. Then, the absorbance values against the concentrations were plotted. The total phenolic substance (TPM) content of the propolis extracts was found according to the graph drawn, and the amount of phenolic substance in the original sample was calculated as mg GAE (Gallic acid equivalent)/100 g propolis by using the dilution factors.

2.4. The total Amount of Flavonoid Substance

Total flavonoid content analysis was performed according to the method of Fukumoto and Mazza (Fukumoto *et al.*, 2000). Different concentrations of quercetin (1; 0.5; 0.25; 0.125; 0.0625; 0.03125 and 0.015625 mg/mL) were used to prepare the standard graph. The amount of flavonoid substance equivalent to quercetin was found according to the graph drawn with the absorbance values at 415nm against the concentration.

2.5. Determination of Total Antioxidant Activity

The FRAP method known as ferric reducing/antioxidant power (Fe(III)-TPTZ-2,4,6-tris(2-pyridyl)-S-triazine) is reduced in the presence of antioxidants and the blue complex Fe(II) is reduced. The formation of TPTZ is based on the maximum absorbance of this complex at 593 nm. The FRAP reagent that gives the method its name was prepared daily. For this purpose, 100 µL of the sample was mixed with 3 mL of FRAP reagent (300 mM pH 3.6 acetate buffer,

10 mM TPTZ, and 20 mM FeCl₃ (10: 1: 1)) and absorbance was read at 593 nm after 4 minutes. Absorbances at 595 nm against the sample-free reference were read at 0 and 4 minutes. Different concentrations of FeSO₄.7H₂O (31.25; 62.5; 125; 250; 500; 1000 μM) were used for calibration. The results were expressed as FeSO₄.7H₂O equivalent antioxidant power (Benzie *et al.*, 1999).

2.6. Synthesis of Silver Nanoparticle Using Propolis Extract

In this process, 10 ml of ethanol extract of propolis was added dropwise to 0.01 M AgNO₃ solution. After stirring for 10 minutes, pH was arranged to 10 by using 1 M NaOH and the solution was stirred until the colour changed from brown to black. Biosynthetic silver nanoparticles were centrifuged at 10.000 rpm for 20 minutes. The precipitated P-AgNPs were washed twice using water and ethanol to remove impurities present on them (Al-Fakeh *et al.*, 2021).

2.7. Characterization Techniques of P-AgNPs Derived from Propolis

Nanoparticles are typically characterized by their size, shape, surface area, and dispersion structure. It is a simple and useful analytical technique to measure the mass concentration of silver nanoparticles obtained by biosynthesis according to Beer's law. It is the technique used to measure the light absorbed and scattered by a sample (Tejamaya *et al.*, 2012).

20 mg of silver nanoparticles obtained by using propolis were taken and mixed with ethyl alcohol/water for half an hour in an ultrasonic bath to ensure complete mixing. It was filtered through the membrane filter in order to remove the aggregate products that may be in the solution containing nanoparticles. Scanning was performed between 200-800 nm using a quartz cell with ethyl alcohol as a reference (UV/Vis-1601, Shimadzu, Kanagawa, Japan).

Attenuated total reflection-Fourier transform infrared (ATR-FTIR) is performed to identify functional groups on nanoparticles. To characterize the functional groups on the synthesized P-AgNPs, measurements were made with 4 cm⁻¹ resolution and 50 scans (PerkinElmer Inc., Norwalk, CT, USA).

Scanning electron microscopy (SEM) based on electron microscopy is a technique used to characterize the morphology of nanoparticles through direct imaging. For SEM analysis, nanoparticles were mixed in ethanol for ten minutes in an ultrasonic bath to prevent aggregation in the medium. The resulting solution was coated with a conductive metal, a gold/palladium alloy, using a spray coater (Zeiss Supra 40 VP, Oberkochen).

EDX analysis is used to characterize nanoparticles synthesized by green synthesis technology. In this method, X-rays are emitted from the nanoparticles after being bombarded by an electron beam. Accordingly, the elemental composition of the nanoparticles can be determined (Quorum Q150R ES, Quorum Technologies Ltd, UK).

The X-ray diffraction (XRD) technique is used to examine the structural information of the metallic nanoparticle. Energetic X-rays can penetrate deep into materials and provide information about the structure. The broadening of the peaks in XRD confirms the formation of nano-sized particles. XRD analyzes (APD 2000 PRO GNR, Novara, Italy) of P-AgNPs were performed using CuK_α radiation and the wavelength of the X-Ray was 1.54059 Å. For silver nanoparticles obtained from propolis, the scanning range was between 2θ= 5-90°, and the measurement was carried out using an integration time of 3 seconds for each angle value. The XRD diffractogram obtained was evaluated semi-quantitatively according to the Match program on the computer connected to the diffractometer and according to the library of ICDD (International Center for Diffraction Data). The average particle size of the synthesized AgNPs was calculated by using the Debye–Scherrer equation.

$$D = \frac{k\lambda}{\beta \cos\theta} \quad (1)$$

where k = shape factor (0.94); λ = X-ray wavelength ($\lambda=1.5418 \text{ \AA}$); β = full width at half maximum (FWHM) in radians; and θ = Bragg's angle.

2.8. Calculation Method

All computations were executed with density functional theory (DFT) at the B3LYP levels of theory with the Gaussian 16 Rev. B01 package (Frisch *et al.*, 2016) and GaussView 6.0.16 (Dennington *et al.*, 2016) was used for visualization of the structure. The compounds were optimized to get the global minimum by using B3LYP/SDD level. The SDD basis sets combine DZ and Stuttgart–Dresden ECP (relativistic effective core potential) basis sets. In our calculations, we tried common basis sets but because of the Ag^+ atoms, we did not succeed the optimizing the molecules. The SDD basis is selected for all molecules. The SDD basis set is the probable quality for the system related to heavy metals which are instrumentally recommended for heavy metals (Tsipis, 2014; Abegg *et al.*, 19741). The absorption spectrum and the excitation energies using the TD-DFT method and natural bond orbital (NBO) analysis in the gas phase, and non-linear optical (NLO) parameters were computed by using the optimized geometry data. The electronic properties and electronic surface potential (ESP) characteristics were achieved from the optimized geometry.

3. RESULTS

Polyphenols with phenolic character, which are found in propolis and produced as secondary metabolites, are in different types and concentrations are agents responsible for antioxidant capacity. Their determination as a total reveals the antioxidant character of the source, they are found in. In addition, the total phenolic substance in natural extracts is important to determine the number of hydroxyl groups that provide antioxidant activity.

The total amount of phenolic substances in propolis by the Folin (Singleton, 1965, Singleton *et al.*, 1999) method, which is based on the formation of a coloured complex with Folin Ciocalteu reagent, is given in Table 1, the total phenolic content of the studied propolis samples was found to be 34.32 mg GAE/g.

It is one of the most frequently used methods to measure the total antioxidant capacity of natural products and extracts. It was first developed by Oyaizu (Oyaizu, 1986) and later modified by Benzie and Strain (Benzie *et al.*, 1999). In addition, the method is simple, fast, and inexpensive compared to other methods applied to determine total antioxidant activity. It is also a method that gives healthy results and does not require any special equipment (Prior *et al.*, 2003). The trolox equivalent of FRAP activities was determined and the values found are given in Table 1. Accordingly, a high FRAP value indicates high antioxidant activity.

Table 1. Total phenolic substance, antioxidant activity, and flavonoid values of propolis samples collected from Mugla-Türkiye.

Sample	Total amount of polyphenol substance (mgGAE/g)	The total amount of flavonoid substance (mg QE/g)	Total antioxidant capacity (Ferric reducing/antioxidant power) FRAP
Liquid ethanolic propolis (s)	34.32±0.44 mgGAE/ ml	10.18±0.06 gGAE/ ml	222.85±1.67 mmol FeSO ₄ .7 H ₂ O/ml

The determination of flavonoids is also called the aluminium chloride colorimetric method, the principle of this method is based on the formation of a stable acid complex of aluminium chloride with the 4-keto and C-3 or C-5 (or both) hydroxyl group of the flavonoids. The total

flavonoid content of ethanolic propolis extracts was found to be 10.18 mg KE/g, and the data obtained are summarized in Table 1.

Propolis, a natural product, is the general name of the sticky substance derived from plant resins by honey bees. Propolis contains various chemical compounds such as polyphenols (flavonoid aglycones, phenolic acids, and their esters, phenolic aldehydes, alcohols, and ketones), sesquiterpene quinones, coumarins, steroids, amino acids, and inorganic compounds. More than 160 compounds have been identified in propolis samples, and these compounds vary according to the botanical and geographic origin of propolis. For example, the main chemical compounds of propolis obtained from poplar trees are flavonoid aglycones, hydroxycinnamic acids, and their esters, while propolis obtained from birch trees contains flavonoid aglycones, *Baccharis* spp. Carbon prenylated derivatives of p-coumaric acid can be given as important active compounds in propolis obtained from (Anklam, 1998).

In this study, the content and amount of polyphenolic and flavonoid compounds in propolis obtained from Muğla-Türkiye were determined according to the Folin-Ciocalteu method (Table 2).

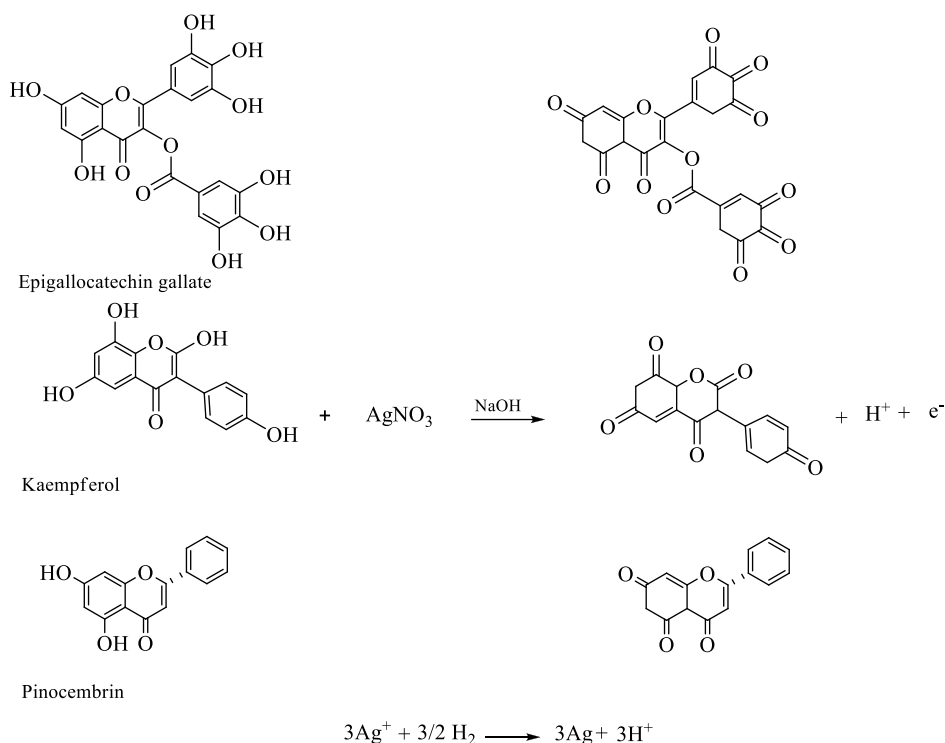
Table 2. Propolis content was obtained from Mugla-Türkiye the region.

Phenolic compounds determined in propolis	Amount ($\mu\text{g/ml}$)
3,4-Dimethoxycinnamic acid	142.16
Apigenin	287.01
Caffeic acid	292.55
Caffeic acid phenethyl ester	2102.26
Chrysin	419.76
Epigallocatechin gallate	24.34
Galangin	959.83
Gallic acid	30.28
Kaempferol	172.73
p-Coumaric acid	116.68
Naringenin	367.28
trans-Cinnamic acid	44.29
trans-Isoferulic acid	225.25
trans-Ferulic acid	86.00
Quercetin	468.02
Pinocembrin	958.08

The synthesis of silver nanoparticles was carried out as an environmentally friendly biosynthesis that does not harm nature, by using these substances in propolis as both reducing and stabilizing agents. It is a fast and simple method since the reaction time required for the formation of particles is shorter and a special system is not required for the reaction. The dark brown colour of propolis turning black as a result of the reaction with the ethanol extract is the first evidence of the formation of P-AgNPs.

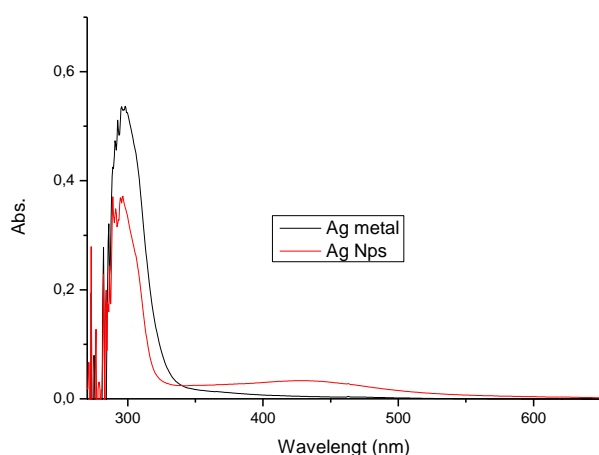
Polyphenols first form a silver complex with the silver ion, and then it is oxidized to the keto form with the release of free electrons and Ag^+ ions formed in the environment. Free electrons formed at the end of the reaction reduce Ag^+ ions to zero-valued silver (Ag^0) (Gautam *et al.*, 2007). At the same time, polyphenol compounds surround the formed silver metals and keep them in the form of nanoparticles (Figure 1).

Figure 1. The silver ions reduced by the phytochemical in the propolis extract are turned into nanoparticles by the stabilizing agent.



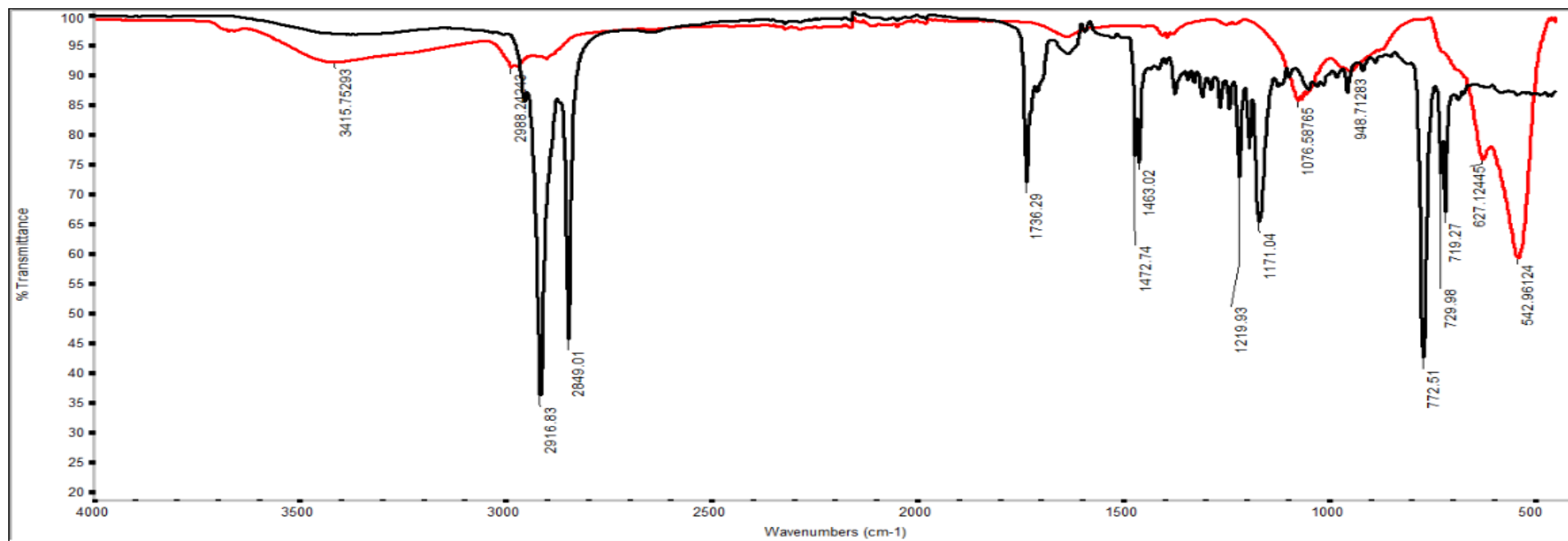
In order to determine the optical properties of silver nanoparticles obtained from the ethyl alcohol extract of propolis, a UV-visible absorption spectrum was taken between 200 and 800 nm. When the absorption spectrum given in [Figure 2](#) is examined, it is seen that P-AgNPs have a maximum absorption at 335 nm (Jain S *et al.*, 2017).

Figure 2. Maximum absorbances of propolis extract and silver nanoparticles in UV visible spectrophotometer.



By comparing the propolis solid and the synthesized P-AgNPs, the FTIR spectrum confidently identifies the functional groups involved in the reaction ([Figure 3](#)). Between wavenumbers 3552 – 4000 cm^{-1} , the broad peak corresponds to the stretching vibration of OH, while the double peak at 2915 cm^{-1} and 2849 cm^{-1} is due to the stretching vibration of CH. The occurrence of too many vibrations between 1500 - 1800 cm^{-1} is an indication of the intense carbonyl groups and the double bonds formed between C atoms and C, N elements. 1472 cm^{-1} , 1210 cm^{-1} are the C–O group of polyols (hydroxy flavonoids), aromatic ether peaks at 1171 cm^{-1} , and the peaks of alkene groups at 772 cm^{-1} .

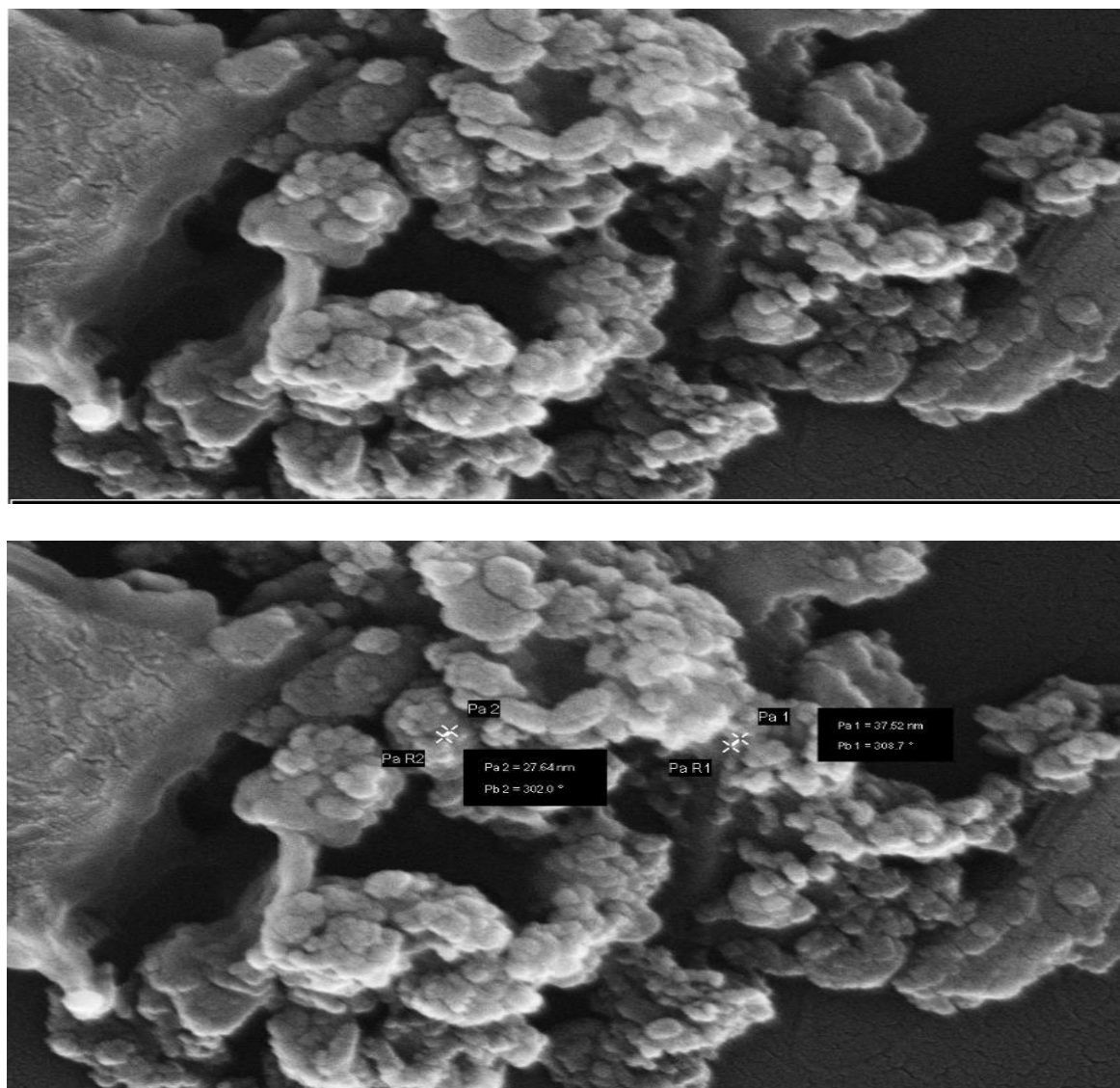
Figure 3. Functional groups attached in silver nanoparticle formation by FT-IR analysis **a.** FT-IR result of propolis extract (black line) **b.** FT-IR result after reaction result after interaction of propolis extract with silver nitrate (red line).



The bands formed in the spectrum of silver nanoparticles are similar to the bands formed in the spectrum of nanoparticles containing propolis. In the spectrum of propolis, the peaks at 2915 and 2849 cm^{-1} and the peaks at cm^{-1} could not be observed in the spectrum of nanoparticles. These peaks are suppressed by broad bands. Apart from this, all other peaks belonging to the propolis extract were also formed in the spectra of the nanoparticles (Lakshman Kumar *et al.*, 2016), the data of AgNPs synthesized by *Echinochloa colona* plant in the green synthesis, and characterization of AgNPs support our research.

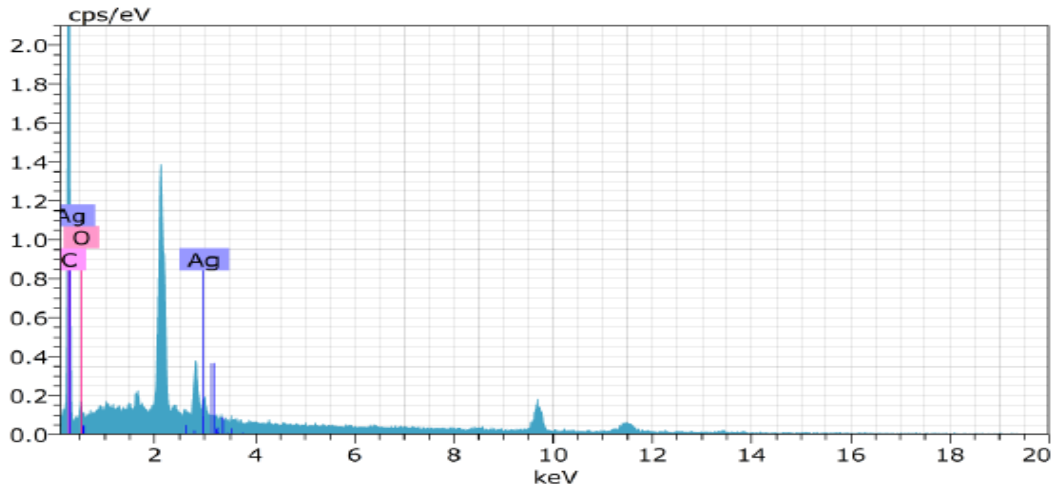
When the FTIR analysis of P-AgNPS is compared with the FTIR analysis of the ethanol extract of propolis, the change in the peaks of polyphenols (phenolics and flavonoids), carboxylic acids, and aromatic and carbonyl compounds is evidence of the formation of AgNPs and that these compounds act as capping agents in nanoparticles.

Figure 4. SEM image of silver nanoparticles produced using propolis extract.



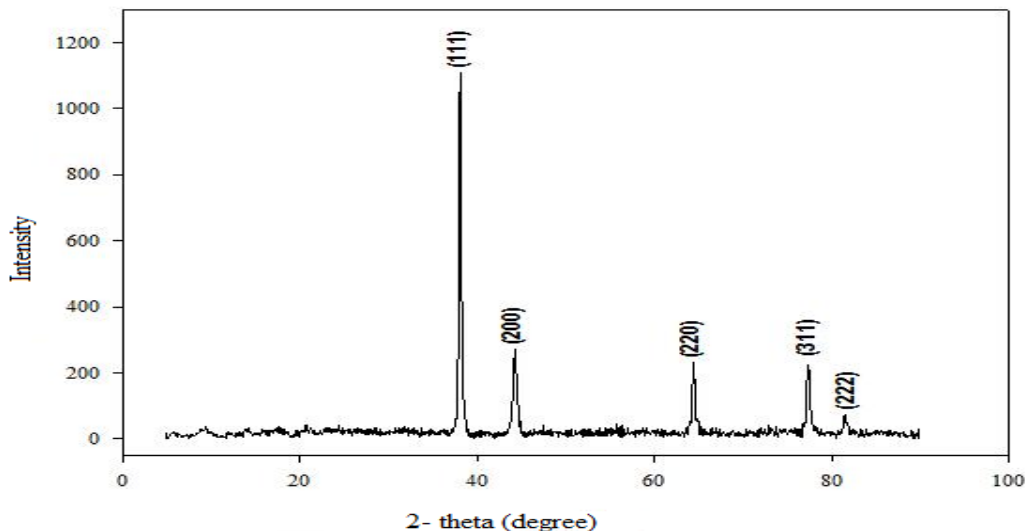
SEM is an important technique used to investigate the surface morphology of nanostructures. SEM images of the biosynthetic P-AgNPs sample are given in Figure 4. It is seen that Ag nanoparticles are randomly dispersed and have sizes ranging from 28 to 34 nm. Normally spherical Ag nanoparticles, which do not have a fully spherical structure in this study, are thought to result from the aggregation of two or more Ag nanoparticles during synthesis. This is in line with other studies in the literature (Dehvari *et al.*, 2018). In the energy-dispersive X-ray spectroscopy (EDX) analysis of the sample shown in Figure 5, 20.4% O and 79.6% Ag elements.

Figure 5. EDX spectroscopy shows the chemical composition of P-AgNPs.



(as atomic) were detected. EDX analyses of AgNPs showed over 79 % silver element as well as low proportions of carbon, oxygen, and nitrogen. Other than silver, other observed signals may have originated from biomolecules around AgNPs (Velammal *et al.*, 2016).

Figure 6. X-ray diffractogram/diffraction patterns of P-AgNPs synthesized using ethanol extract of propolis.

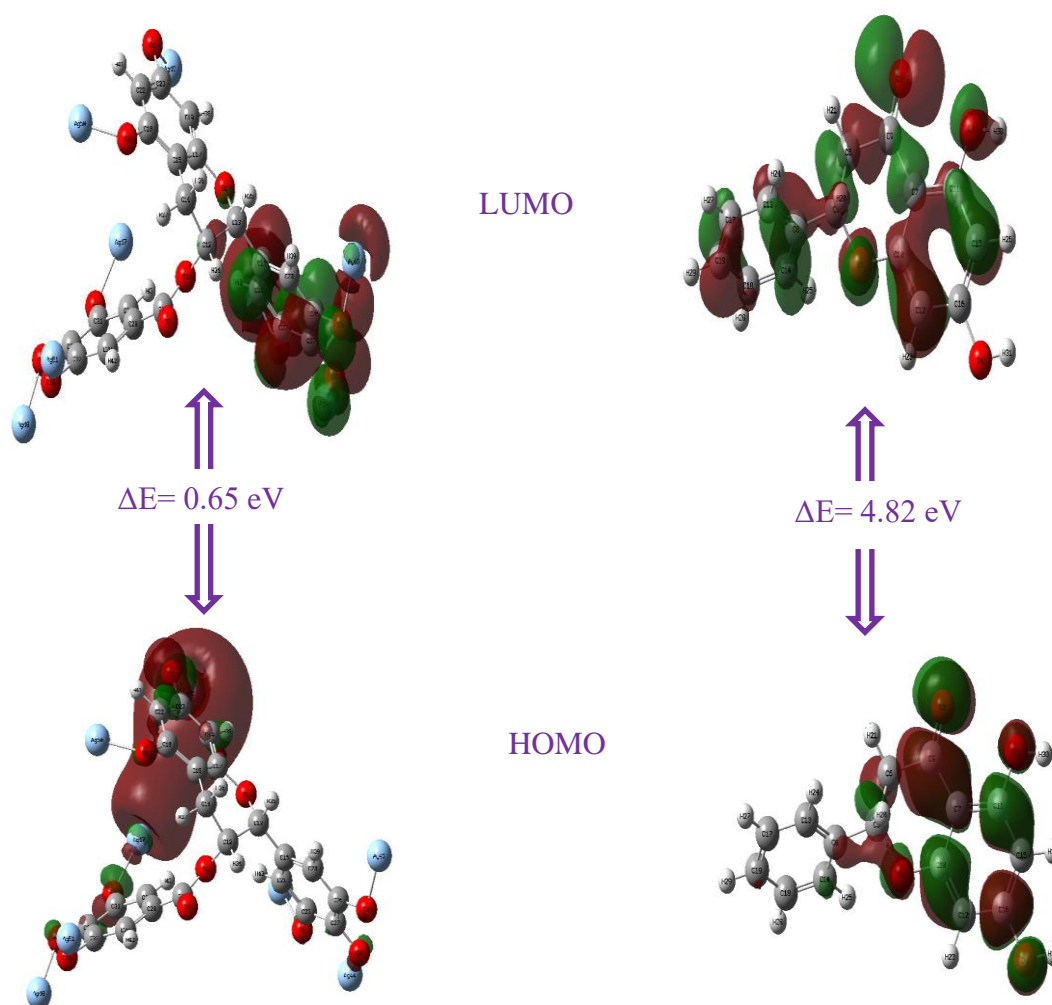


The powder XRD spectrum of the P-AgNPs sample is given in Figure 6 at angles of 27, 30, 34, 56, 37, 86, 46, 10, 64, 32 and 77.02 (2θ) originating from Ag nanoparticles; 2.67; 2.37; 1.97; Characteristic peaks corresponding to (222), (111), (200), (220) and (311) diffractions with distances of 1.44 and 1.24 Å were observed (JCPDS card no 04-0783). The positions and intensities of the obtained peaks indicate that Ag nanoparticles are face-centred cubic (Jasrotia *et al.*, 2020).

3.1. Electronic Properties

Quantum mechanical molecular orbital calculations give information about the transition state and active site for the reactions. The molecule which has a small energy difference between the HOMO and the LUMO orbitals represents the reactivity of the molecule, holding the two molecules in position for reaction, and also these molecules are called soft molecules (Stevens *et al.*, 2017).

Figure 7. Molecular orbitals diagram of Epigallocatechin gallate + Ag⁺.



The value of the electronic descriptors calculated by Koopmans' theorem using the energy of the HOMO and the LUMO orbitals are given in Table 3. From Table 3, the polyphenols are more stable than the polyphenols binding with Ag⁺ and also, and the most reactive molecule is the Epigallocatechin gallate + Ag⁺ which has huge binding energy with the value of 0.65 eV and is also a soft molecule. Pinocembrin has low chemical reactivity and high kinetic stability with a value of 4.82 eV (Fukui, 1982).

The distribution of the molecular orbitals is very similar for all of the molecules shown in Figure 7 like pinocembrin except Epigallocatechin gallate + Ag⁺. Due to the electron delocalization between C-C bonds ($\pi^*-\pi^*$ interactions), as will be mentioned in Section Natural Bond Analysis, HOMO-LUMO orbitals show a distribution as shown in Figure 7.

Table 3. Electronic descriptors of the phenols.

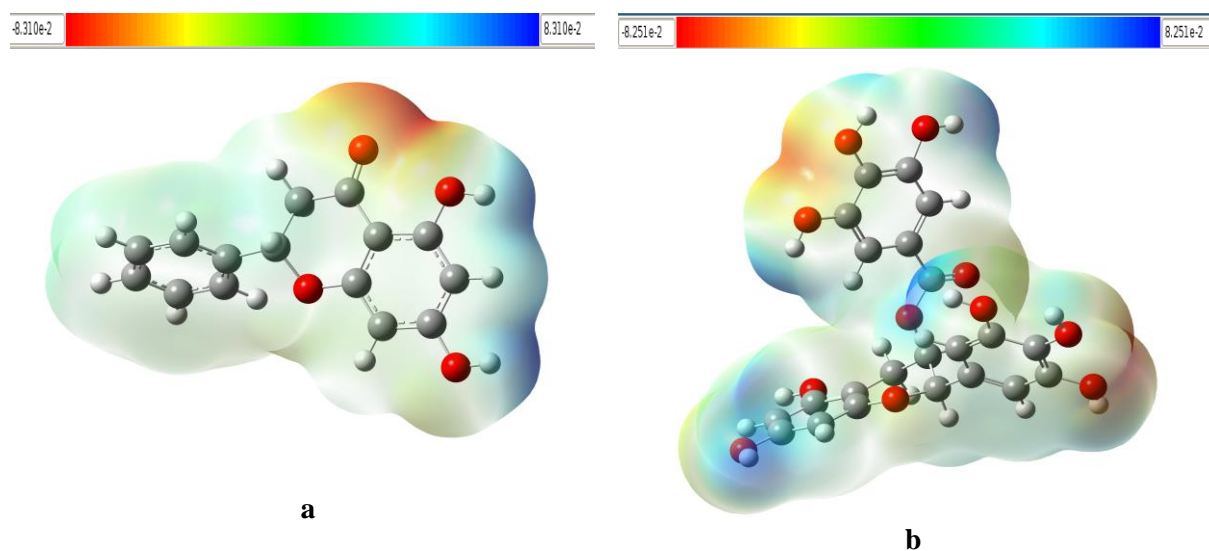
Phenols	Electronic descriptors of the phenols										Electronic descriptors at the end of the reaction of the phenols with Ag ⁺									
	E _{HOMO}	E _{LUMO}	ΔE	I	A	χ	η	s	μ	ω	E _{HOMO}	E _{LUMO}	ΔE	I	A	χ	η	s	μ	ω
3,4-Dimethoxycinnamic acid	-6.09	-2.10	3.99	6.09	2.1	4.10	1.99	0.50	-4.10	4.20	-5.79	-3.15	2.64	5.79	3.15	4.47	1.32	0.76	-4.47	7.57
Apigenin	-6.35	-2.36	3.99	6.35	2.36	4.36	1.99	0.50	-4.36	4.75	-4.76	-3.92	0.84	4.76	3.92	4.34	0.42	2.38	-4.34	22.42
Caffeic acid	-6.26	-2.21	4.05	6.26	2.21	4.24	2.03	0.49	-4.24	4.43	-5.36	-3.83	1.53	5.36	3.83	4.60	0.77	1.31	-4.60	13.80
Caffeic acid phenethyl ester	-6.16	-2.05	4.11	6.16	2.05	4.11	2.06	0.49	-4.11	4.10	-5.51	-3.99	1.52	5.51	3.99	4.75	0.76	1.32	-4.75	14.84
Chrysin	-6.44	-2.46	3.98	6.44	2.46	4.45	1.99	0.50	-4.45	4.96	-5.04	-3.70	1.34	5.04	3.7	4.37	0.67	1.49	-4.37	14.25
Epigallocatechin gallate	-5.91	-1.77	4.14	5.91	1.77	3.84	2.07	0.48	-3.84	3.56	-4.31	-3.66	0.65	4.31	3.66	3.99	0.33	3.08	-3.99	24.43
Galangin	-6.24	-2.37	3.87	6.24	2.37	4.31	1.94	0.52	-4.31	4.79	-4.65	-3.59	1.06	4.65	3.59	4.12	0.53	1.89	-4.12	16.01
Gallic acid	-6.49	-1.79	4.7	6.49	1.79	4.14	2.35	0.43	-4.14	3.65	-4.47	-3.55	0.92	4.47	3.55	4.01	0.46	2.17	-4.01	17.48
Kaempferol	-6.18	-2.30	3.88	6.18	2.3	4.24	1.94	0.52	-4.24	4.63	-4.53	-3.59	0.94	4.53	3.59	4.06	0.47	2.13	-4.06	17.54
p-Coumaric acid	-6.36	-2.19	4.17	6.36	2.19	4.28	2.09	0.48	-4.28	4.38	-5.25	-3.87	1.38	5.25	3.87	4.56	0.69	1.45	-4.56	15.07
Naringenin	-6.27	-1.64	4.63	6.27	1.64	3.96	2.32	0.43	-3.96	3.38	-5.00	-3.66	1.34	5	3.66	4.33	0.67	1.49	-4.33	13.99
trans-Cinnamic acid	-6.74	-2.30	4.44	6.74	2.3	4.52	2.22	0.45	-4.52	4.60	-6.34	-3.23	3.11	6.34	3.23	4.79	1.56	0.64	-4.79	7.36
trans-Isoferulic acid	-6.11	-2.14	3.97	6.11	2.14	4.13	1.99	0.50	-4.13	4.29	-5.07	-3.24	1.83	5.07	3.24	4.16	0.92	1.09	-4.16	9.43
trans-Ferulic acid	-6.26	-2.16	4.1	6.26	2.16	4.21	2.05	0.49	-4.21	4.32	-5.00	-3.35	1.65	5.00	3.35	4.18	0.83	1.21	-4.18	10.56
Quercetin	-6.17	-3.78	2.39	6.17	3.78	4.98	1.20	0.84	-4.98	10.36	-4.73	-3.78	0.95	4.73	3.78	4.26	0.48	2.11	-4.26	19.06
Pinocembrin	-6.46	-1.64	4.82	6.46	1.64	4.05	2.41	0.41	-4.05	3.40	-5.12	-3.73	1.39	5.12	3.73	4.43	0.70	1.44	-4.43	14.09

*The phenols were randomly numbered from 1 to 16.

3.2. Molecular Electrostatic Potential Analysis

Electrostatic surface potential (ESP) is a useful facility for cognizance of where the electron distribution effect is regnant. ESP maps demonstrate the positive, negative, and neutral electrostatic potential regions in different colors. Areas with a negative electrostatic surface associated with the electronegative atom pair are shown in red. As seen in Figure 8, the most reactive parts of the compound are around the O atoms with the highest electron density, while the stable parts are in the C-H regions with the lowest electron density.

Figure 8. ESP maps of **a.** Epigallocatechin gallate, **b.** Pinocembrin.



3.3. Binding Energy

The binding energy of Ag^+ is calculated as the given formula below;



As seen in Table 4, the binding energy of Ag^+ to phenolics per atom is close to each other.

Table 4. The binding energies of Ag to the molecules (phenolics).

Num*	Phenolics	E_b (eV)	The Amount of phenolic compounds in propolis (mg/ml)
1	3,4-Dimethoxycinnamic acid	-21.4802	142.16
2	Apigenin	-23.5707	287.01
3	Caffeic acid	-24.0351	292.55
4	Caffeic acid phenethyl ester	-22.2552	2102.26
5	Chrysin	-22.3378	419.76
6	Epigallocatechin gallate	-28.8121	24.34
7	Galangin	-23.9137	959.83
8	Gallic acid	-26.5054	30.28
9	Kaempferol	-25.0347	172.73
10	p-Coumaric acid	-22.3906	116.68
11	Naringenin	-23.5788	367.28
12	trans-Cinnamic acid	-21.4298	44.29
13	trans-Isoferulic acid	-22.4824	225.25
14	trans-Ferulic acid	-22.4848	86.00
15	Quercetin	-26.5538	468.02
16	Pinocembrin	-22.9139	958.08

*The phenolics were randomly numbered from 1 to 16.

The molecular electrostatic potential has been used to foretell the reactive sides of the molecule and hydrogen bonding interactions as well as their potential use in biological recognition studies (Murray *et al.*, 1996; Scrocco *et al.*, 1978). Also, Figure 8 pointed out the electrostatic potential surfaces of Epigallocatechin gallate and Pinocembrin which have the highest and the lowest binding energy. The red regions show the nucleophilic and the blue regions show the electrophilic surfaces of the compounds.

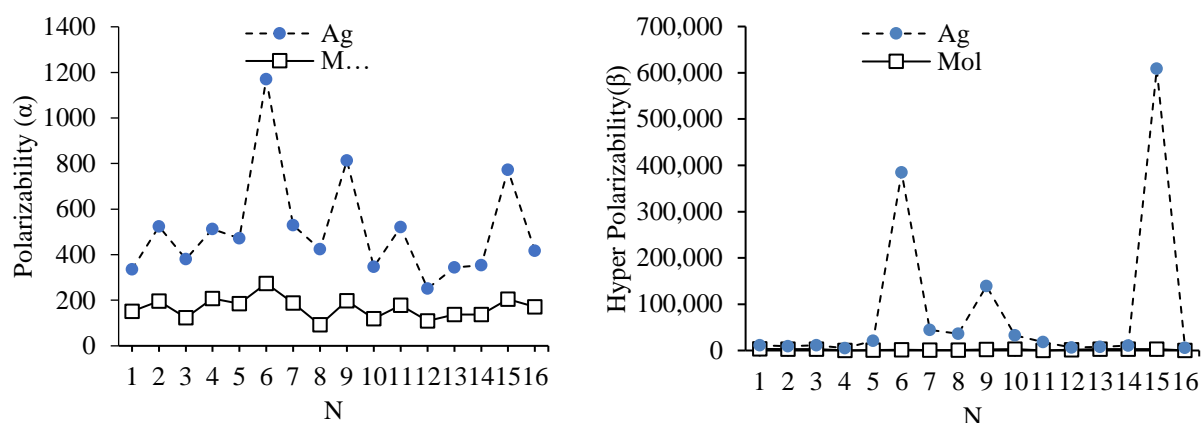
3.4. Optical Properties

Polarizability is another significant characteristic of the electronic property of a molecule (Eşme *et al.*, 2014), DFT is used to compute the parameters such as; dipole moment (μ_t), the mean polarizability ($\langle\alpha\rangle$), and the total first static hyperpolarizability (β_t) for the title molecule. The parameters μ_t and $\langle\alpha\rangle$ are connected with the first and higher-order derivatives of the electron density (Kleinman, 1962; Pipek *et al.*, 1989).

The magnitude of the molecular hyperpolarizability β is one of the key factors in the non-linear optical (NLO) system. The dipole moment (μ), mean polarizability (α), and first hyperpolarizability (β) values of the phenols have been computed at B3LYP/SDD level in the gas phase and solvent, respectively, and are presented in Table 5. The first static hyperpolarizability β values have been calculated as 12.541×10^{-30} in the solvent and 5.160×10^{-30} in the gas phase. The polarizability and the hyperpolarizability values have increased from the gas phase to the solvent phase. It can be said that this is due to stabilizing the polarized excited state of the molecule via solvent and/or hydrogen bonding and allowing the intramolecular charge transfer to occur more efficiently in the solvent. Usually, Urea is used as a prototypical molecule to determine the NLO properties of the molecular system (Prashanth *et al.*, 2015). The μ_t and β_t values for the title compound have been calculated as 5.0831 debye and 5.160×10^{-30} esu, whereas the references values for Urea are 1.3732 debye and 0.3728×10^{-30} esu, respectively. Thus, it appears that the total dipole moment and total first-order hyperpolarizability values of the molecule are greater than those of Urea.

Table 5. Dipole moment, Polarizability, and Hyper Polarizability values of the phenolic compounds in gas and in DMSO.

Num Compounds	Gas			DMSO			
	Dipole Moment	Polarizability (α)	Hyper Polarizability (β)	Dipole Moment	Polarizability (α)	Hyper Polarizability (β)	
	Mol	Mol	Mol	Ag	Ag	Ag	
1	3,4-Dimethoxycinnamic acid	5.8	151.3	3419.7	1.9	184.3	7598.2
2	Apigenin	3.8	196.5	3023.8	3.7	327.6	6458.3
3	Caffeic acid	5.5	123.7	2704.4	3.2	257.1	8895.3
4	Caffeic acid phenethyl ester	5.1	207.3	207.3	6.1	305.0	4689.3
5	Chrysin	4.1	185.3	1194.5	8.3	286.5	19966.0
6	Epigallocatechin gallate	3.6	274.0	1707.8	6.4	896.3	382923.5
7	Galangin	5.3	188.1	799.6	8.4	340.5	43470.9
8	Gallic acid	2.6	92.2	1121.0	6.4	332.4	34829.2
9	Kaempferol	4.8	198.0	2445.0	4.8	615.1	137152.4
10	p-Coumaric Acid	3.8	119.6	2750.5	4.6	226.9	30222.6
11	Naringenin	4.0	178.0	562.5	3.9	343.0	17822.7
12	trans-Cinnamic acid	2.9	109.7	1396.7	1.7	141.7	4838.1
13	trans-Isoferulic acid	6.3	137.8	3237.3	5.2	206.1	4467.9
14	trans-Ferulic acid	4.4	137.0	2911.7	5.4	216.5	7665.1
15	Quercetin	6.0	204.3	3047.6	1.3	567.6	605591.2
16	Pinosembrin	2.9	171.3	568.4	4.8	245.3	5503.3

Figure 9. The alteration of the NLO properties to molecules in the extract.

*N: 16 molecules were found in the extract and these molecules were randomly numbered from 1 to 16.

The average polarizability and hyperpolarizability values of the phenols considered in the propolis content were calculated. After these molecules were bound with Ag, a very large increase in the values of molecules Epigallocatechin gallate, Kaempferol, and Quercetin was calculated. It can be said that after the binding of these molecules with Ag, the NLO properties increase even more. The results are illustrated in Figure 9.

3.5. Natural Bond Orbital Analysis

The charge transfer in the molecule in addition to intramolecular interaction is verified by natural bond orbital (NBO) analysis. To examine the interactions between occupied and virtual orbitals of a system, the DFT method has been used to foretell the delocalization of electrons (Karthick *et al.*, 2011; Arivazhagan *et al.*, 2012; Govindarajan *et al.*, 2012). NBO analysis (Weinhold, 1998), involving the deletion of matrix elements corresponding to the CO bonding/antibonding orbital as well as lone pair/antibonding orbital interactions expands upon recent work that investigated stereoelectronic contributions to gauche stabilization through analysis of NBO $E^{(2)}$ transfer energies (Trindle *et al.*, 2003). The $E^{(2)}$ value indicates the interaction energy between electron acceptor and electron donors and this value is great for the addition of electrons donation from donor to acceptor.

The results of the NBO analysis of the Epigallocatechin gallate and its compound binding with Ag are obtained at B3LYP/SDD level presented in Table 6 and Table 7, respectively. The hyper-conjugative $\sigma \rightarrow \sigma^*$ interactions play an extremely significant role in the molecule and represent the weak departures from a strictly localized natural Lewis structure that constitutes the primary 'noncovalent' effects (Dege *et al.*, 2014).

Table 6 shows that the strongest stabilization energy in Epigallocatechin gallate is calculated as 370.09 kcal/mol between π^* (C31 – C33) \rightarrow π^* (C28 - C30). Also, the interaction between π^* (O7 - C24) \rightarrow π^* (C28 - C30) has 67.95 kcal/mol giving the structure a strong stabilization. Table 7 shows that the strongest stabilization energy in Epigallocatechin gallate + Ag⁺ is calculated as 270.61 kcal/mol between π^* (C20 - C26) \rightarrow π^* (C16 - C21). The interactions between π^* (C18 - C22) \rightarrow π^* (C15 - C17) has 252.50 kcal/mol, π^* (C31 – C33) \rightarrow π^* (C28 – C30) has 234.33 kcal/mol, π^* (C19 – C23) \rightarrow π^* (C15 – C17) has 175.68 kcal/mol and π^* (C25 – C27) \rightarrow π^* (C16 – C21) 164.47 kcal/mol also give the structure a strong stabilization.

Table 6. Remarkable stabilization interactions for the Epigallocatechin gallate.

Donor (i)	Type	ED/e	Acceptor (j)	Type	ED/e	E ⁽²⁾ (kcal/mol)
C15 - C17	π	1.68291	C15 - C17(π^*)	π^*	0.41195	1.57
			C18 - C22 (π^*)	π^*	0.40266	26.04
			C19 - C23(π^*)	π^*	0.40495	15.58
C16 - C20	π	1.71476	C21 - C25(π^*)	π^*	0.41169	17.42
			C26 - C27(π^*)	π^*	0.43158	22.19
C19 - C23	π	1.70563	C18 - C22 (π^*)	π^*	0.40266	25.73
			C15 - C17(π^*)	π^*	0.41195	24.66
			C18 - C22(π^*)	π^*	0.40266	14.59
C21 - C25	π	1.69289	C16 - C20(π^*)	π^*	0.41445	22.14
			C26 - C27(π^*)	π^*	0.43158	19.02
C26 - C27	π	1.62880	C16 - C20(π^*)	π^*	0.41445	19.44
			C21 - C25(π^*)	π^*	0.41169	23.30
C28 - C30	π	1.67577	O7 - C24 (π^*)	π^*	0.28410	26.40
			C29 - C32 (π^*)	π^*	0.38507	19.50
			C31 - C33 (π^*)	π^*	0.43423	21.52
C29 - C32	π	1.69421	C28 - C30 (π^*)	π^*	0.43818	19.74
			C31 - C33 (π^*)	π^*	0.43423	19.94
C31 - C33	π	1.60567	C28 - C30 (π^*)	π^*	0.43818	21.79
			C29 - C32 (π^*)	π^*	0.38507	21.81
O3	LP 2	1.88900	C18 - C22 (π^*)	π^*	0.40266	25.35
O4	LP 2	1.88882	C19 - C23 (π^*)	π^*	0.40495	25.78
O5	LP 2	1.90626	C21 - C25(π^*)	π^*	0.41169	21.67
O6	LP 2	1.88634	C26 - C27(π^*)	π^*	0.43158	24.53
O7	LP 2	1.85759	O2 - C24 (σ^*)	sp ^{2.35}	0.10635	32.22
			C24 - C28 (σ^*)	sp ^{1.52}	0.05845	15.00
O8	LP 2	1.87858	C26 - C27 (π^*)	π^*	0.43158	25.80
O9	LP 2	1.88497	C31 - C33(π^*)	π^*	0.43423	24.52
O10	LP 2	1.90539	C29 - C32 (π^*)	π^*	0.38507	22.06
O11	LP 2	1.86151	C31 - C33 (π^*)	π^*	0.43423	27.47
O7 - C24 (π^*)	π^*	0.28410	C28 - C30 (π^*)	π^*	0.43818	67.95
C31 - C33 (π^*)	π^*	0.43423	C28 - C30 (π^*)	π^*	0.43818	370.09

Table 7. Remarkable stabilization interactions for the Epigallocatechin gallate + Ag⁺.

Donor (i)	Type	ED/e	Acceptor (j)	Type	ED/e	E ⁽²⁾ (kcal/mol)
C15 - C17	π	1.66666	C18 - C22	π^*	0.43457	25.78
			C19 - C23	π^*	0.44531	15.30
C16 - C21	π	1.69508	C20 - C26	π^*	0.40437	16.24
			C25 - C27	π^*	0.46256	20.78
C18 - C22	π	1.97078	C15 - C17	π^*	0.41651	15.49
			C18 - C22	π^*	0.43457	1.41
			C19 - C23	π^*	0.44531	27.02
C19 - C23	π	1.97150	C15 - C17	π^*	0.41651	25.02
			C18 - C22	π^*	0.43457	13.69
C20 - C26	π	1.69804	C16 - C21	π^*	0.41511	22.75
			C25 - C27	π^*	0.46256	15.44
C25 - C27	π	1.53472	C16 - C21	π^*	0.41511	22.40
			C20 - C26	π^*	0.40437	18.52
C28 - C30	π	1.67799	O7 - C24	π^*	0.30377	28.94
			C29 - C32	π^*	0.38098	18.91
			C31 - C33	π^*	0.02676	18.97
C29 - C32	π	1.72177	C28 - C30	π^*	0.45446	18.65
			C31 - C33	π^*	0.02676	16.54
C31 - C33	π	1.50483	C28 - C30	π^*	0.45446	24.04
			C29 - C32	π^*	0.38098	19.17
O1	LP(2)	1.87072	C15 - C17	π^*	0.41651	22.64
O2	LP(2)	1.82316	O7 - C24	π^*	0.30377	37.43
O3	LP(2)	1.85532	C18 - C22	π^*	0.43457	19.23
O4	LP(2)	1.86700	C19 - C23	π^*	0.44531	18.57
O6	LP(2)	1.84433	C20 - C26	π^*	0.40437	15.34
O6	LP(3)	1.63801	C20 - C26	π^*	0.44531	14.38
			O2 - C24	$sp^{2.48}$	0.10338	31.38
			C12 - C13	$sp^{2.57}$	0.02505	0.79
O7	LP(2)	1.86535	C24 - C28	$sp^{1.48}$	0.05627	13.97
			C26 - C27	$sp^{1.88}$	0.06113	10.75
O8	LP(2)	1.81321	C26 - C27	$sp^{1.88}$	0.06113	10.75
O8	LP(3)	1.66667	C25 - C27	π^*	0.46256	43.12
O9	LP(2)	1.86446	C31 - C33	π^*	0.02676	12.18
O9	LP(3)	1.64243	C31 - C33	π^*	0.02676	14.13
O11	LP(3)	1.67832	C31 - C33	π^*	0.02676	34.81
O7 - C24	π^*	0.30377	C28 - C30	π^*	0.45446	56.43
C18 - C22	π^*	0.43457	C15 - C17	π^*	0.41651	252.50
C19 - C23	π^*	0.44531	C15 - C17	π^*	0.41651	175.68
C20 - C26	π^*	0.44531	C16 - C21	π^*	0.41511	270.61
C25 - C27	π^*	0.46256	C16 - C21	π^*	0.41511	164.47
C31 - C33	π^*	0.02676	C28 - C30	π^*	0.45446	234.33

4. DISCUSSION and CONCLUSION

Among metal nanoparticles, AgNPs have attracted great interest for many years due to their unique optical (SPR), electrical and physicochemical properties. They can be synthesized easily and can be obtained as monodisperse in a narrow particle size range. The synthesis of AgNPs by the green synthesis method, which is carried out using various biological sources such as plants and bacteria, draws attention to the fact that toxic chemicals are not used and it is an environmentally friendly method. First, the polyphenols in the ethanol/water extract of propolis were determined and the synthesis of silver nanoparticles was successfully carried out. It has been found by theoretical studies that Epigallocatechin gallate, Kaempferol, and Quercetin compounds in propolis are effective in the synthesis of silver nanoparticles.

Since the energy difference between the orbitals of the molecules formed by the interaction of Epigallocatechin gallate, Apigenin, Gallic acid, Kaempferol, and Quercetin molecules with Ag^{+1} is quite low, they are more reactive and soft molecules than other molecules.

As a result, it was calculated that phenolic molecules Epigallocatechin gallate, Kaempferol, and Quercetin with high NLO values bind better with Ag^{+1} . Therefore, these compounds are effective in obtaining nano-Ag. At the same time, Epigallocatechin gallate, Kaempferol, and Quercetin phenolics with high NLO properties are thought to be worth examining as organic optical technological materials.

Acknowledgments

The authors are also grateful to Pamukkale University (Grant numbers: 2018FEBE002 and 2020FEBE012) and TUBITAK ULAKBIM, High Performance and Grid Computing Center (TRUBA Resources).

Declaration of Conflicting Interests and Ethics

The authors declare no conflict of interest. This research study complies with research and publishing ethics. The scientific and legal responsibility for manuscripts published in IJSM belongs to the authors.

Authorship Contribution Statement

Aslı Ozturk Kiraz: Investigation, resources, visualization, theoretical calculation, formal analysis, and writing - original draft. **Mine Sulak:** Methodology, supervision, validation and analyses to be performed. **Yesim Kara:** Investigation, resources and preparation of propolis extract. **Izzet Kara:** Methodology, supervision, theoretical calculation, formal analysis.

Orcid

Aslı Ozturk Kiraz  <https://orcid.org/0000-0001-9837-0779>

Mine Sulak  <https://orcid.org/0000-0003-1300-8661>

Yesim Kara  <https://orcid.org/0000-0002-7027-3667>

Izzet Kara  <https://orcid.org/0000-0002-9837-2819>

REFERENCES

- Abegg, P.W., Ha, T.K. (1974). Ab initio calculation of spin-orbit-coupling constant from Gaussian lobe SCF molecular wavefunctions. *Molecular Physics*, 27, 763-767. <https://doi.org/10.1080/00268977400100661>
- Al-Fakeh, M.S., Osman, S.O.M., Gassoumi M., Rabhi M., Omer, M. (2021). Characterization, antimicrobial and anticancer properties of palladium nanoparticles biosynthesized optimally using Saudi propolis. *Nanomaterials*, 11, 2666. <https://doi.org/10.3390/nano11102666>
- Anklam, E. (1998). A review of the analytical methods to determine the geographical and botanical origin of honey. *Food Chemistry*, 63, 549–562. [https://doi.org/10.1016/S0308-8146\(98\)00057-0](https://doi.org/10.1016/S0308-8146(98)00057-0)

- Arivazhagan, M., Kavitha, R. (2012). Molecular structure, vibrational spectroscopic, NBO, HOMO-LUMO and Mulliken analysis of 4-methyl-3-nitro benzyl chloride. *Journal of Molecular Structure*, 1011, 111-120. <https://doi.org/10.1016/j.molstruc.2011.12.006>
- Benzie, I.F., Strain, J.J. (1999). Ferric reducing/antioxidant power assay: direct measure of total antioxidant activity of biological fluids and modified version for simultaneous measurement of total antioxidant power and ascorbic acid concentration. *Methods Enzymol.*, 299, 15–27. [https://doi.org/10.1016/s0076-6879\(99\)99005-5](https://doi.org/10.1016/s0076-6879(99)99005-5)
- Bhattacharya, R., Mukherjee, P. (2008). Biological properties of “naked” metal nanoparticles. *Advanced Drug Delivery Reviews*, 60(11), 1289-1306. <https://doi.org/10.1016/j.addr.2008.03.013>
- Das, R., Nath, S.S., Chakdar, D., Gope, G., Bhattacharjee, R. (2009). Preparation of silver nanoparticles and their characterization. *Journal of Nanotechnology*, 5, 1-6.
- Dege, N., Senyüz, N., Batu, H., Günay, N., Avcı, D., Tamer, Ö., Atalay, Y. (2014). The synthesis, characterization and theoretical study on nicotinic acid [1-(2,3-dihydroxyphenyl) methylidene)hydrazide. *Spectrochim Acta A Mol. Biomol. Spectrosc.*, 120, 323–331. <https://doi.org/10.1016/j.saa.2013.10.030>
- Dehvari, M., Ghahghaei, A. (2018). The effect of green synthesis silver nanoparticles (AgNPs) from *Pulicaria undulata* on the amyloid formation in α -lactalbumin and the chaperon action of α -casein. *International Journal of Biological Macromolecules*, 108, 1128-1139. <https://doi.org/10.1016/j.ijbiomac.2017.12.040>
- Dennington, R., Keith, T.A., Millam, J.M. (2016). *GaussView*, Version 6. (Shawnee Mission KS, Semichem Inc.
- Eşme, A., Sağdıncı, S.G. (2014). The linear, nonlinear optical properties and quantum chemical parameters of some sudan dyes. *J BAUN Inst. Sci. Technol.*, 16(1), 47-75.
- Frisch, M.J., Trucks, G.W., Schlegel, H.B., Scuseria, G.E., Robb, M.A., Cheeseman, J.R., ... & Fox, D.J. (2016). Gaussian 16, Revision C.01, Gaussian, Inc., Wallingford CT.
- Fukui, K. (1982). Role of frontier orbitals in chemical reactions. *Science*, 218, 747– 754. <https://doi.org/10.1126/science.218.4574.747>
- Fukumoto L.R., Mazza G. (2000) Assessing antioxidant and prooxidant activities of phenolic compounds. *J. Agric. Food Chem.*, 48, 3597-3604. <https://doi.org/10.1021/jf000220w>
- Gautam, A, Singh, G.P., Ram, S. (2007). A simple polyol synthesis of silver metal nanopowder of uniform particles. *Synth. Met.*, 157, 5-10. <https://doi.org/10.1016/j.synthmet.2006.11.009>
- Geethalakshmi, R., Sarada, D.V. (2012). Gold and silver nanoparticles from *Trianthema decandra*: synthesis, characterization, and antimicrobial properties. *Int. J. Nanomedicine*, 7, 5375-5384. <https://doi.org/10.2147/IJN.S36516>
- Govindarajan, M., Karabacak, M., Suvitha, A., Periandy, S. (2012). FT-IR, FT-Raman, ab initio, HF and DFT studies, NBO, HOMO-LUMO and electronic structure calculations on 4-chloro-3-nitrotoluene. *Spectrochimica Acta Part A: Molecular and Biomolecular Spectroscopy*, 89, 137-148. <https://doi.org/10.1016/j.saa.2011.12.067>
- Hojat, V., Azizi, S., Mohammadi, P. (2018). Green synthesis of the silver nanoparticles mediated by thymra spicata extract and its application as a heterogeneous and recyclable nanocatalyst for catalytic reduction of a variety of dyes in water. *Journal of Cleaner Production*. 170, 1536-1543. <https://doi.org/10.1016/j.jclepro.2017.09.265>
- Jain, S., Mehata, M.S. (2017). Medicinal plant leaf extract and pure flavonoid mediated green synthesis of silver nanoparticles and their enhanced antibacterial property. *Scientific Reports*, 7(1), 15867. <https://doi.org/10.1038/s41598-017-15724-8>
- Jasrotia, T., Chaudhary, S, Kaushik, A., Kumar, R., Chaudhary, G.R. (2020). Green chemistry-assisted synthesis of biocompatible Ag, Cu, and Fe₂O₃ nanoparticles. *Materials Today Chemistry*, 15, 100214. <https://doi.org/10.1016/j.mtchem.2019.100214>

- Karthick, T., Balachandran, V., Perumal, S., Nataraj, A. (2011). Rotational isomers, vibrational assignments, HOMO-LUMO, NLO properties and molecular electrostatic potential surface of N-(2-bromoethyl) phthalimide. *Journal of Molecular Structure*, 1005, 202–213. <https://doi.org/10.1016/j.molstruc.2011.08.051>.
- Kleinman, D.A. (1962) Nonlinear Dielectric Polarization in Optical Media. *Physical Review*, 126, 1977-1979. <https://doi.org/10.1103/PhysRev.126.1977>
- Krell, R. (1996). *Value-Added Products from Beekeeping*. Fao Agricultural Services Bulletin No. 124 Chapter 3, Pollen.
- Lakshman Kumar, D., Siva Sankar, S., Venkatesh, P., Hepcy Kalarani, D. (2016). Green synthesis of silver nanoparticles using aerial parts extract of *Echinochloa colona* and their characterization. *European J. Pharm. Med. Res.*, 3(4), 325-328.
- Mason, S.E., Iceman, C.R., Trainor, T.P., Chaka, A.M. (2010). Molecular-level understanding of environmental interfaces using density functional theory modeling. *Physics Procedia*, 4, 67–83. <https://doi.org/10.1016/j.phpro.2010.08.010>
- Murray, J.S., & Sen, K. (1996). *Molecular Electrostatic Potentials, Concepts and Applications*. Elsevier.
- Oyaizu, M. (1986). Studies on product of browning reaction prepared from glucose amine. *Jpn. J. Nutr. Diet.*, 44, 307-315. <https://doi.org/10.5264/eiyogakuzashi.44.307>
- Padil, V.V.T., Cernik, M. (2013). Green synthesis of copper oxide nanoparticles using gum karaya as a biotemplate and their antibacterial application. *International Journal of Nanomedicine*, 8, 889-898. <https://doi.org/10.2147/IJN.S40599>
- Petri, G., Lemberkovics, E., & Foldvari, M. (1988). *Examination of Differences Between Propolis (Bee Glue) Produced from Different Floral Environments*. In: Flavours and Fragrances: a world perspective. Lawrence, B.M., Mookherjee, B.D., Willis, B.J. (Eds.) Elsevier Sci. Publ., Amsterdam, pp 439-446.
- Pipek, J., Mezey, P.Z. (1989). A fast intrinsic localization procedure applicable for ab initio and semiempirical linear combination of atomic orbital wave functions. *The Journal of Chemical Physics*, 90, 4916. <https://doi.org/10.1063/1.456588>
- Prashanth, J., Ramesh, G., Naik, J., Ojha, J., Reddy, B., Rao, G. (2015). Molecular structure, vibrational analysis and first order hyperpolarizability of 4-Methyl-3-Nitrobenzoic Acid using density functional theory. *Optics and Photonics Journal*, 5, 91-107. <https://doi.org/10.4236/opj.2015.53008>
- Prior, R.L., Hoang, H., Gu, L., Wu, X., Bacchocca, M., Howard, L., Hampsch-Woodill, M., Huang, D., Ou, B., Jacob, R. (2003). Assays for hydrophilic and lipophilic antioxidant capacity (oxygen radical absorbance capacity (ORAC_{FL})) of plasma and other biological and food samples. *J. Agric. Food. Chem.*, 51, 3273-3279. <https://doi.org/10.1021/jf0262256>
- Ramnath, S. (2017). Synthesis of copper nanoparticles from bee propolis extract and its antibacterial property. *European J. Pharm. Med. Res.*, 4, 684-688.
- Santhoshkumar, J., Venkat, Kumar, S., Rajeshkumar, S. (2017). Synthesis of zinc oxide nanoparticles using plant leaf extract against urinary tract infection pathogen. *Resource-Efficient Technologies*, 3(4), 459-465. <https://doi.org/10.1016/j.refit.2017.05.001>
- Scrocco, E., Tomasi, J. (1978). Electronic molecular structure, reactivity and intermolecular forces: an euristic interpretation by means of electrostatic molecular potentials. *Advances in Quantum Chemistry*, 11, 115–121. [https://doi.org/10.1016/S0065-3276\(08\)60236-1](https://doi.org/10.1016/S0065-3276(08)60236-1)
- Siddiquee, M.A., Ud din Parray, M., Mehdi, S.H., Alzahrani, K.A., Alshehri, A.A., Malik, M.A., Patel, R. (2020). Green synthesis of silver nanoparticles from delonix regia leaf extracts: in-vitro cytotoxicity and interaction studies with bovine serum albumin. *Materials Chemistry and Physics*, 242, 122493. <https://doi.org/10.1016/j.matchemphys.2019.122493>
- Singleton, V.L., & Rossi, J.A. (1965) Colorimetry of Total Phenolics with Phosphomolybdic-Phosphotungstic Acid Reagent. *American Journal of Enology and Viticulture*, 16, 144-158.

- Singleton, V.L., Orthofer, R., Lamuela-Raventos, R.M. (1999). Analysis of total phenols and other oxidation substrates and antioxidants by means of folin-ciocalteu reagent. *Methods in Enzymology*, 299, 152-178. [http://dx.doi.org/10.1016/S0076-6879\(99\)99017-1](http://dx.doi.org/10.1016/S0076-6879(99)99017-1)
- Slinkard, K., Singleton, V.L. (1977). Total phenol analysis: automation and comparison with manual methods. *American Journal of Enology and Viticulture*, 28(1), 49-55.
- Stevens, J. (2017). Virtually going green: The role of quantum computational chemistry in reducing pollution and toxicity in chemistry. *Physical Sciences Reviews*, 2(7), 20170005. <https://doi.org/10.1515/psr-2017-0005>
- Tejamaya, M., Roemer, I., Merrifield, R.C., Lead, J.R. (2012). Stability of citrate, PVP, and PEG coated silver nanoparticles in ecotoxicology media. *Environ. Sci. Technol.*, 46, 7011-7017. <https://doi.org/10.1021/es2038596>
- Trindle, C., Crum, P., Douglass, K. (2003). G2(MP2) Characterization of Conformational Preferences in 2-Substituted Ethanol (XCH₂CH₂OH) and Related Systems. *J. Phys. Chem. A*, 107, 6236. <https://doi.org/10.1021/jp034598j>
- Tsipis, A.C. (2014). DFT flavor of coordination chemistry. *Coordination Chemistry Reviews*, 272, 1–29. <https://doi.org/10.1016/j.ccr.2014.02.023>
- Van Mourik, T., Bühl, M., Gaigeot, M.P. (2014). Density functional theory across chemistry, physics, and biology. *Philosophical Transactions of the Royal Society A*, 372, 20120488. <https://doi.org/10.1098/rsta.2012.0488>
- Velammal, S.P., Devi, T.A., Amaladhas, T.P. (2016). Antioxidant, antimicrobial and cytotoxic activities of silver and gold nanoparticles synthesized using *Plumbago zeylanica* bark. *Journal of Nanostructure in Chemistry*, 6, 247-260. <https://doi.org/10.1007/s40097-016-0198-x>
- Weinhold, F. (1998). Natural Bond Orbital Methods In: *Encyclopedia of Computational Chemistry* 3, John Wiley and Sons.